

Successive Multipole Order Transitions of the Spin–Orbit-Coupled Metal $\text{Cd}_2\text{Re}_2\text{O}_7$

The 5d pyrochlore oxide superconductor $\text{Cd}_2\text{Re}_2\text{O}_7$ (CRO) has attracted significant interest as a spin–orbit-coupled metal (SOCM) that undergoes odd-parity multipole transitions due to strong spin–orbit interaction. We have conducted ultra-high resolution synchrotron x-ray diffraction experiments on a high-quality CRO single crystal. The temperature dependence of allowed and forbidden reflections in the high-temperature cubic phase I reveals that the previously believed first-order transition between phase II and III consists of two close second-order transitions; there is a new orthorhombic phase XI in between. Each phase is believed to correspond to a distinct odd-parity multipole order, and the complex successive transitions observed may be the result of switching of odd-parity multipole phases.

In general, the Fermi surfaces of metals become unstable against various interactions, and characteristic ordered states appear to resolve them. Recently, Fu proposed the concept of spin–orbit-coupled metal (SOCM), considering the Fermi liquid instability originating from spin–orbit interaction (SOI) [1]. The Fermi liquid instability in SOCM induces spontaneous inversion symmetry breaking (ISB), resulting in odd parity ordering of itinerant electrons. Such odd-parity multipole order induces novel transport properties such as magnetocurrent effect and nonreciprocal transport under a magnetic field, which may be useful for future applications [2].

The pyrochlore oxide superconductor $\text{Cd}_2\text{Re}_2\text{O}_7$ (CRO) has garnered considerable interest as a promising SOCM candidate [3]. CRO undergoes spontaneous ISB transition at $T_{s1} \sim 200$ K from cubic phase I to tetragonal phase II. Although the tetragonal deformation at T_{s1} is very small ($\sim 0.10\%$), the electronic state changes drastically with a sharp decrease in electrical resistivity and a nearly 50% decrease in density of states [3]. Therefore, the ISB transition is considered to be an electronic phase transition driven by the Fermi liquid instability of SOCM [1, 3]. In addition, there is another phase transition at $T_{s2} \sim 120$ K from phase II to a different tetragonal structure without inversion symmetry (phase III) [3].

Phase II and III are suggested to correspond to odd parity multipole orders predicted for SOCM [1]. As depicted in Fig. 1 (a), the displacements of Re atoms in phase II and III can be viewed as electric dipoles, certain pairs of which generate electric toroidal moments. These virtual electric toroidal moments are organized as $x^2 - y^2$ and $3z^2 - r^2$ configurations, respectively [4]. Thus, the emerged electronic orders are regarded as electric toroidal quadrupole (ETQ) orders [2]. Since these ETQ orders cannot switch continuously, the phase transition between phase II and III at T_{s2} was considered to be of the first order.

Crystal structure is very important for understanding the emergent electronic phases and the origin of electronic phase transitions. However, crystal structures of CRO reported so far have been contradicting.

We performed high-resolution synchrotron radiation x-ray diffraction (XRD) experiments on a high-quality CRO crystal to elucidate the intrinsic structural changes. Recent improvements in crystal quality resulted in a one order of magnitude increase in residual resistivity ratio and allowed the observations of quantum oscillations [4, 5].

Figure 1 (c) shows representative XRD patterns at four distinct phases of CRO. In phase I, the $0\ 0\ 16_c$ reflection is observed as a single peak, while the $0\ 0\ 14_c$ reflection is absent. In phase II, the $0\ 0\ 16_c$ reflection splits into two peaks and two similar peaks appear around the $0\ 0\ 14_c$ reflection. In phase III at the lowest temperature, two peaks are observed at the $0\ 0\ 16_c$ reflection location and one at the $0\ 0\ 14_c$ reflection location. Compared to phase II, the intensity of the high and low angle peaks has been reversed. Thus, the tetragonal distortion has been reversed between phase II and III. A diffraction pattern clearly distinguishable from phases II and III was observed at $T = 110$ K. Three peaks were observed at both reflection locations. This new phase is designated as phase XI; to date, ten phases, including the high-pressure phases, have been reported [3]. In terms of symmetry, phase XI, which is continuously connected to $I\bar{4}m2$ (phase II) and $I4_122$ (phase III), is likely $F222$. Relationship between the unit cell axes of the four phases of CRO are shown in Fig. 1 (b) and the temperature dependence of the lattice constants obtained in this study is summarized in Fig. 1 (d). The previously believed first-order transition between phase II and III was found to consist of two close second-order transitions at $T_{s2} = 115$ K and $T_{s3} \sim 100$ K.

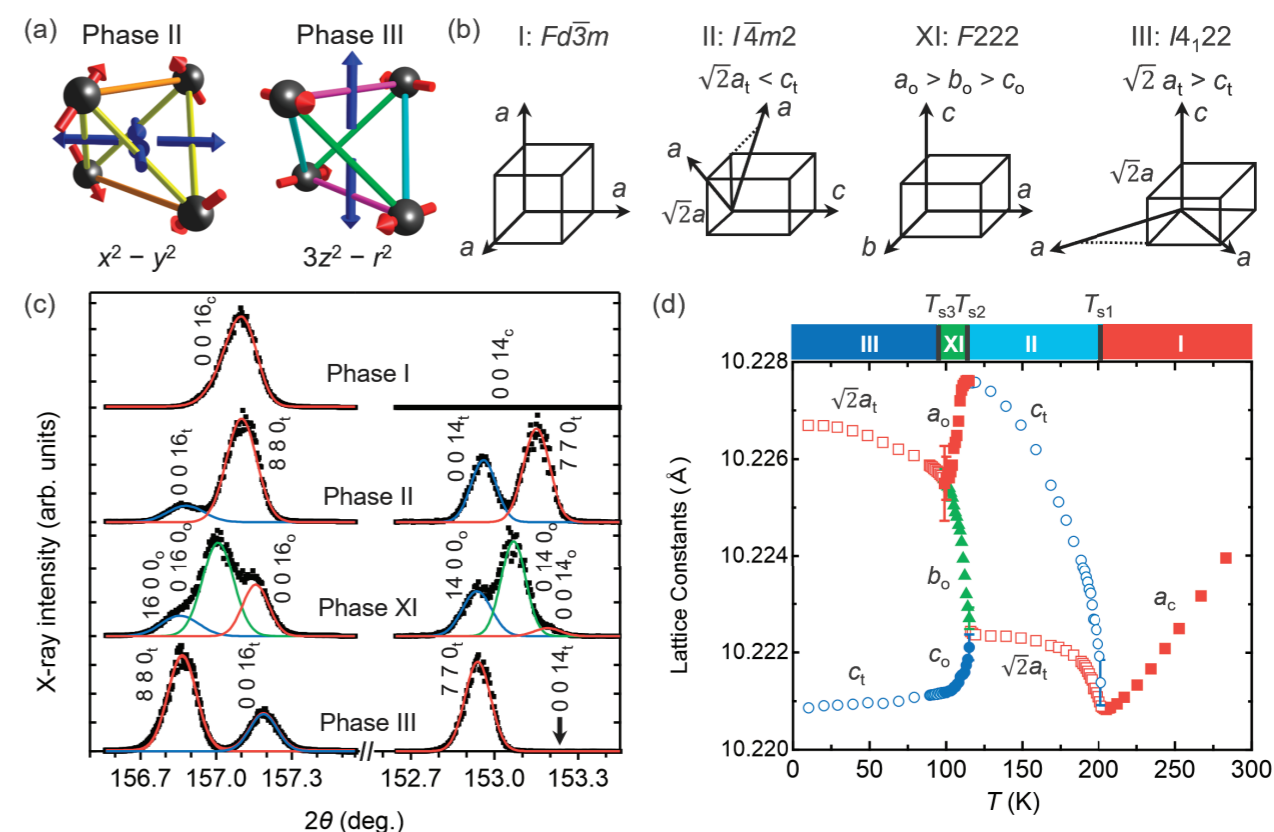


Figure 1: (a) Schematic figure of the deformation of Re tetrahedron in phases II and III, with red arrows representing the displacements of Re atoms (black balls). The Re displacements generate virtual electric toroidal moments (blue arrows) of the $x^2 - y^2$ and $3z^2 - r^2$ types, respectively. The colors of the connecting rods between Re atoms differentiate identical bonds in each phase. (b) Relationship between the unit cell axes of the four phases of $\text{Cd}_2\text{Re}_2\text{O}_7$. (c) Representative XRD patterns of a multidomain single crystal of $\text{Cd}_2\text{Re}_2\text{O}_7$ containing the $0\ 0\ 16_c$ and $0\ 0\ 14_c$ reflections in phase I (at 252 K), II (at 149 K), XI (at 110 K), and III (at 10 K). The curves that best fit a single Gaussian or multiple skew-normal distribution functions are represented by solid lines. The peak indices are based on cubic, tetragonal, orthorhombic, and tetragonal unit cells, respectively. (d) Temperature dependences of lattice constants for $\text{Cd}_2\text{Re}_2\text{O}_7$.

The order parameter (OP) of the I–II–III successive phase transitions is understood in terms of a two-dimensional irreducible representation of E_u [6]. The E_u OP is represented by the two-dimensional vector. In phase II, only one component has a finite value, whereas in phase III, only the other has a finite value. The OP of phase XI is the linear combination of the two components. It is therefore reasonable that phase XI is continuously linked to phases II and III. The II–XI–III successive phase transitions can be regarded as a switching of ETQ from $x^2 - y^2$ to $3z^2 - r^2$ type through a linear combination of them.

Consequently, we determined the temperature dependence of the lattice constants and the space group for each phase [7]. The most significant discovery is a new orthorhombic phase XI overlooked for years in between two close second-order transitions at T_{s2} and T_{s3} . Our findings may advance understanding of the microscopic origin of the odd-parity multipoles in CRO and the characteristics of SOCM.

REFERENCES

- [1] L. Fu, *Phys. Rev. Lett.* **115**, 026401 (2015).
- [2] S. Hayami, Y. Yanagi, H. Kusunose and Y. Motome, *Phys. Rev. Lett.* **122**, 147602 (2019).
- [3] Z. Hiroi, J. Yamaura, T.C. Kobayashi, Y. Matsubayashi and D. Hirai, *J. Phys. Soc. Jpn.* **87**, 024702 (2018).
- [4] H. T. Hirose, T. Terashima, D. Hirai, Y. Matsubayashi, N. Kikugawa, D. Graf, K. Sugii, S. Sugiura, Z. Hiroi and S. Uji, *Phys. Rev. B* **105**, 035116 (2022).
- [5] Y. Matsubayashi, D. Hirai, M. Tokunaga and Z. Hiroi, *J. Phys. Soc. Jpn.* **87**, 104604 (2018).
- [6] I. A. Sergienko and S. H. Curnoe, *J. Phys. Soc. Jpn.* **72**, 1607 (2003).
- [7] D. Hirai, A. Fukui, H. Sagayama, T. Hasegawa and Z. Hiroi, *J. Phys.: Condens. Matter* **35**, 035403 (2023).

BEAMLIN

BL-4C

D. Hirai¹, A. Fukui², H. Sagayama³, T. Hasegawa⁴ and Z. Hiroi² (¹Nagoya Univ., ²ISSP, ³KEK-IMSS, ⁴Hiroshima Univ.)